

Estimation of Groundwater and Salinity for the Central Biscayne Bay Coast, Florida, USA

Vladimir J. Alarcon[1(✉)], Anna C. Linhoss[2], Paul F. Mickle[3], Christopher R. Kelble[4], and Alexandra Fine[4]

[1] Civil Engineering Department, Universidad Diego Portales, 441 Ejercito Av., Santiago, Chile
vladimir.alarcon@udp.cl

[2] Department of Biosystems Engineering, Auburn University, 3101, Shelby Center, Auburn, AL 36849, USA
alinhoss@auburn.edu

[3] Northern Gulf Institute, 1021 Balch Blvd., Stennis Space Center, Starkville, MS 39529, USA
pmickle@ngi.msstate.edu

[4] NOAA Atlantic Oceanographic and Meteorological Laboratory, 4301 Rickenbacker Causeway, Miami, FL 33149, USA
{chris.kelble,alexandra.fine}@noaa.gov

Abstract. Estimating groundwater flows in karst-dominated landscapes is difficulted by the lack of observed groundwater flows and the uncertainty in hydrogeological parameters (hydraulic conductivity, specific storage and yield, porosity, anisotropy, etc.). The State of Florida (USA) landscape is dominated by the largest geographic area of geologically young carbonate and rocks with well-developed karst features in North America. In this research, a MODFLOW groundwater model for central Biscayne Bay is presented. The Bay is surrounded by karst terrain. The groundwater model is loosely linked to a hydrodynamic model to estimate salinity concentrations at the Biscayne Bay's central coast. The loose-link model framework is shown to improve salinity estimations in 50% from estimations that do not include groundwater contributions to the Bay. A statistical comparison of simulated concentrations versus observed data demonstrates that the loose-link model simulates salinity concentration values and trends within acceptable margin of errors ($0.72 < R < 0.77$; $0.52 < R^2 < 0.59$; $0.62 < K\text{-}G < 0.70$; $d > 0.76$; $4.1\% < PBIAS < 13.5\%$). These results have the potential to be applied to other coastal locations in Florida and the world where karst terrain is predominant.

Keywords: Biscayne Bay · Groundwater · Salinity · Southeast Florida · Karst · Aquifer · MODFLOW

1 Introduction

Karst landscapes cover 7–12% of Earth's continental area, and approximately 25% of the world's population partially or completely relies on drinking water from karst aquifers

© The Author(s), under exclusive license to Springer Nature Switzerland AG 2022
O. Gervasi et al. (Eds.): ICCSA 2022 Workshops, LNCS 13379, pp. 594–606, 2022.
https://doi.org/10.1007/978-3-031-10545-6_40

[1]. Therefore, knowledge of the effects of surface and groundwater flow through karst terrain is paramount for optimizing regional water resources use.

The global percentage of land covered by karst soils is distributed unevenly in the world: Europe (23.54%), Middle East and Central Asia (20.97%), East and Southeast Asia (18.27%), the Russian Federation Plus (17.87%), North America (16.31%), Africa (10.49%), Australia (6.81%), and South America (4.31%) [2]. In the United States extensive carbonate karst occurs in Mississippian and Ordivican age limestones (Fig. 1). The southeastern United States has extensive carbonate karst in Florida, Alabama, and Georgia [2].

Florida landscape is dominated by the largest geographic area of geologically young carbonate and rocks with well-developed karst features in North America (Fig. 1) and it is a one of the largest karst areas in the world. [3]. Because of the abundant pore space in Florida's karst terrain, water movement occurs through fractures and other secondary openings (highly permeable conduits). This double set of open pore spaces and high permeability results in the high productivity of the aquifers.

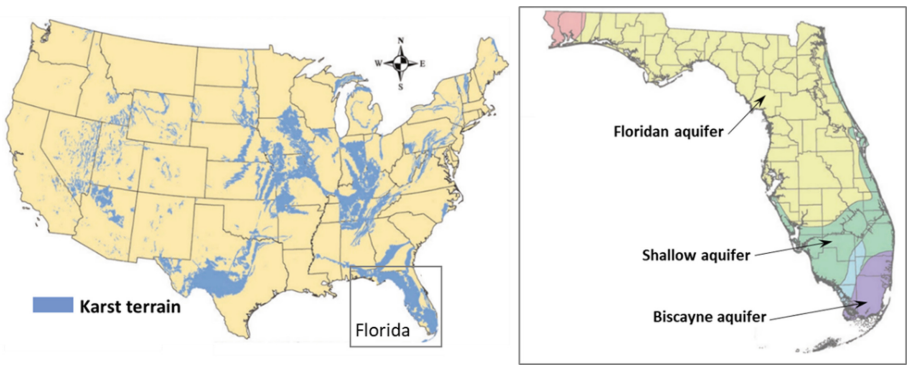

Fig. 1. Karst terrain in North America and main karst aquifers in Florida (USA) (modified from [3]).

The zone of karst-dominated landscape in Florida correlates with areas of unconfined and semi-confined conditions of the Floridan Aquifer [4]. Unconfined aquifers feed fresh water to the Northern Gulf of Mexico and the Atlantic Ocean. Coastal aquifers are an important freshwater resource for significant portions of the global population. Understanding the dynamic relationship between aquifer recharge, storage and discharge is fundamental for sustainable groundwater management [5].

In coastal locations where groundwater produces low salinity zones, estimating the salinity regime at the coast has implications for biological communities and for urban settlements [6]. A recent modeling study on the hydrodynamic regime and salinity spatial distribution in Biscayne Bay (Southeast Florida, USA) was able to replicate salinity concentration values and seasonal trends occurring within the bay [7]. In this study, salinity estimations were poorest for locations close to the coast, especially during the wet season. Unknown groundwater flow sources seem to be lowering salinity concentrations at the coast. Also, freshwater flow to the Florida Northern Gulf of Mexico is

greatly enhanced by the substantial groundwater contributions from aquifer base flow [8]. Estimating groundwater flow in the Florida peninsula would not only positively impact management of water resources, but also would help characterizing salinity regime at the Florida coasts.

The United States Geological Service's Modular Three-dimensional Finite-difference Groundwater Flow Model (MODFLOW) has been applied in the past to quantify groundwater contributions to South Florida coasts. However, those estimations were not used to explore the effect of groundwater flow in salinity concentrations.

This research presents a MODFLOW groundwater model developed to estimate groundwater contributions to the central coast of Biscayne Bay, Florida, USA. The model-estimated flows are introduced into a hydrodynamic/salinity model of the bay to quantify salinity concentrations in the coastal waters at Biscayne Bay.

2 Methods

2.1 Study Area

Biscayne Bay (an oligotrophic water body) receives land-based flows from the Miami metro area. It is located in southeast Florida (adjacent to the Miami metropolitan area) covering an area of approximately 700 km^2 (Fig. 2).

The water depth in the bay ranges between 1.8 m and 4 m, except in dredged areas where depths can exceed 12 m [9]. The Biscayne Bay area includes the largest marine national park in the U.S. national park system: Biscayne National Park, an important part of the recreational, social, economic, and cultural life of Southeast Florida [10].

The Biscayne aquifer underlies the area surrounding Biscayne Bay, it extends beneath the Bay, and also underlies the near shore of the Atlantic Ocean. The aquifer consists of highly permeable interbedded limestone and sandstone. These highly permeable rocks are covered in most places only by a thin layer of porous soil. The aquifer is wedge-shaped and ranges in thickness from 0.6 m on its western edge, to more than 100 m toward the coast [11].

Most of the geologic formations comprising the aquifer are of Pleistocene age but, locally, Pliocene rocks also are included in the aquifer. Its water table is a subdued replica of the land surface, meaning that the water table is at a higher altitude under hills and at a lower altitude under valleys. The water table fluctuates rapidly in response to variations in recharge (precipitation), natural discharge, and pumping from well fields (common in southeast Florida). Natural discharge is by seepage (into streams, canals, or the ocean), and evapotranspiration [12].

The geology and lithology of the Biscayne aquifer are dominated by sand layers at the surface and carbonates and minor sandstone layers at greater depth. This is important from a hydrodynamic point of view. These types of fractured and karstic rocks facilitate the formation of far-reaching regional groundwater flow systems even at the moderate elevation differences of less than 10 m between recharge and discharge areas [13].

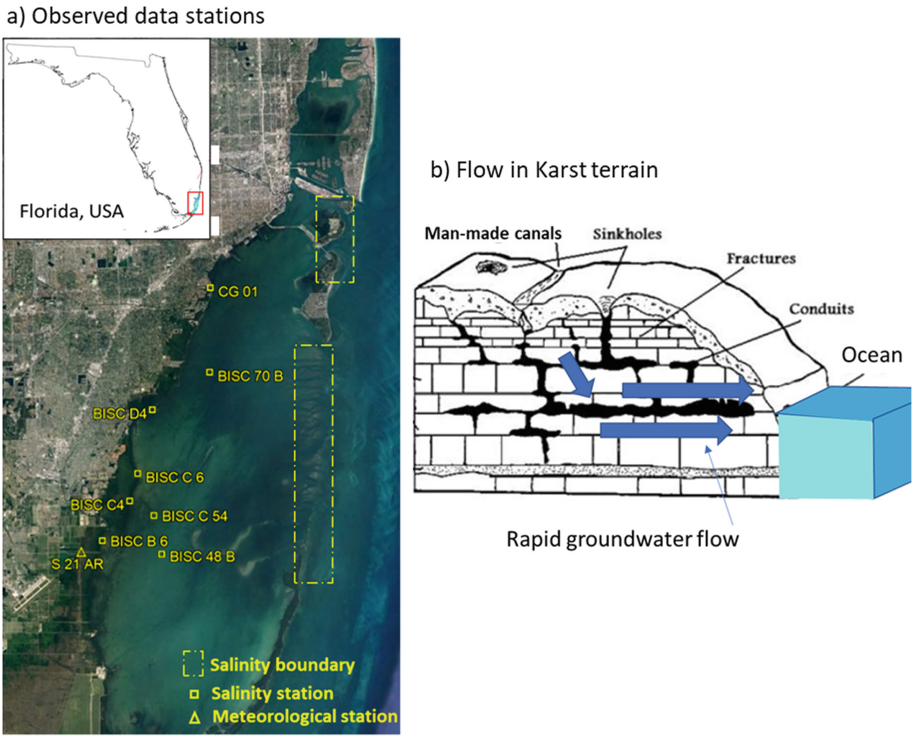

Fig. 2. Study area. a) Biscayne Bay and location of salinity stations in the Bay and salinity boundary conditions. The meteorological station (S21AR) is also shown. b) Flow in karst terrain: sinkholes, fractures, and preferential flow conduits promote rapid groundwater flow to the ocean.

Figure 2 shows the location of salinity stations in the Biscayne Bay. Three salinity stations located in the central coast (BISC C4, BISC C6, BISC D4) are chosen in this research as representative of the coastal salinity regime in the central coast. Hourly salinity concentration data collected at those stations were used in this research.

2.2 Meteorology

Salinity in estuarine systems is influenced by climate and weather. The climate in Southeast Florida is characterized by hot and humid rainy summer, and mild winters (Fig. 3). The annual average minimum, mean, and maximum temperatures in the area are 15 °C, 26 °C, and 32 °C, respectively, and the total annual precipitation average is 1507 mm. The total annual average potential evapotranspiration (ETP) loss in the area ranges from 1220 mm to 1320 mm per year. Stalker et al. [14] estimated a freshwater input ratio canal/precipitation/groundwater of 37%:53%:10% in the wet season, and 40%:55%:5% in the dry season, with an error of ±25%. Approximately 75% of the total precipitation falls in the wet season, generating substantial run-off.

Figure 3 shows precipitation and potential evapotranspiration data from Miami Airport meteorological station that were used to implement meteorological forcings to the

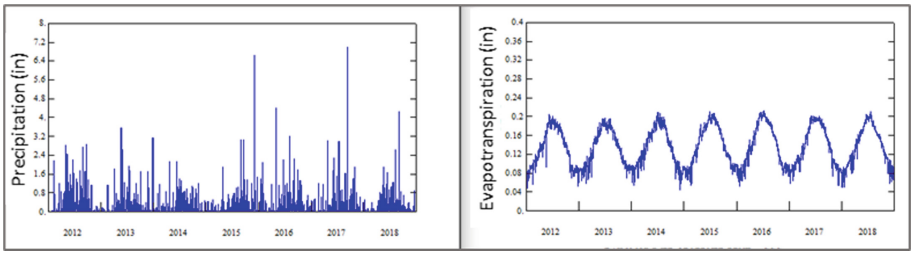

Fig. 3. Precipitation and potential evapotranspiration in Southeast Florida. Data from meteorological station S21AR (see Fig. 2) are shown.

groundwater model of central Biscayne Bay. As shown in the figure, years 2015 to 2017 were the rainiest years within 2012–2018 time period. In those years (2015–2017), the strongest effect of freshwater inputs in salinity were observed. For that reason, those years were used for groundwater flow simulation and subsequent coastal salinity simulation via an existing hydrodynamic and salinity model (detailed in [15]).

2.3 MODFLOW Groundwater Model Development

This section details the procedure for developing a groundwater flow MODFLOW application for central Biscayne Bay.

Aquifer Limits Delineation

Topographical data from the US National Elevation Dataset (NED) was used to delimit the boundaries of the Biscayne aquifer that drain into central Biscayne Bay.

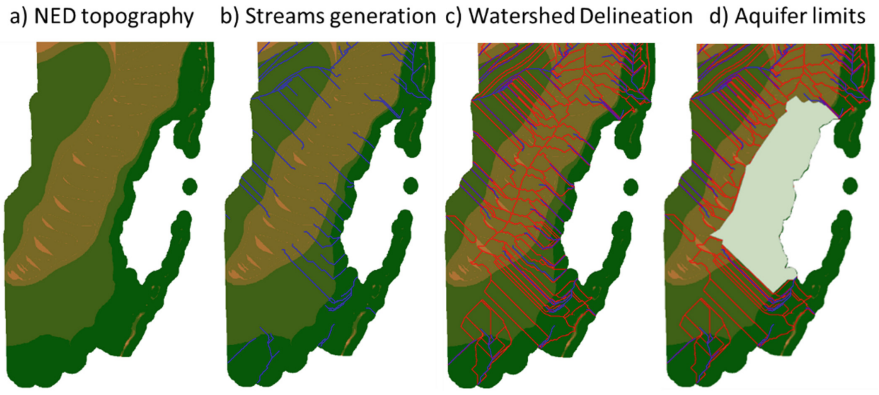

Fig. 4. Delimitation of the inland aquifer. a) NED topography used to delimit inland areas that drain into central Biscayne Bay, b) stream digitalization based on topography, c) watershed delineation to identify areas that drain to Biscayne Bay, and d) topographical mask that delimits the Biscayne aquifer in coastal Biscayne Bay. It is assumed that groundwater recharge area is similar to surface water drainage area.

Since groundwater in an unconfined aquifer is gravity driven, watershed delineation of surface waters gives a good estimate of the area of the inland aquifer that feeds groundwater to the Bay. Figure 4 illustrates the use of NED topography to delimit the inland aquifer boundaries that feed freshwater to central Biscayne Bay. Standard hydrological geoprocessing was performed to generate the geographical boundaries: stream generation, watershed delineation, and merging of all surface watershed areas that drain to central Biscayne Bay into a mask. The NED topographical layer was intersected with the mask and a topographical raster for the aquifer was produced. This raster was used to develop the corresponding MODFLOW model for groundwater flow simulation.

MODFLOW Model

The development of the groundwater model was performed using ModelMuse: a graphical user interface (GUI) for the U.S. Geological Survey MODFLOW [16]. In ModelMuse, the spatial data for the model are independent of the grid, and the temporal data are independent of the stress periods [16]. The topographical raster representing the inland aquifer was the basic data for defining recharge areas and model output locations.

The MODFLOW computational grid consists of a structured non-curvilinear mesh (Fig. 5) consisting of 3 layers, and 6500 active cells. Each active cell is of 300 m × 300 m. Horizontal isotropy was enforced and vertical hydraulic conductivity was defined as one

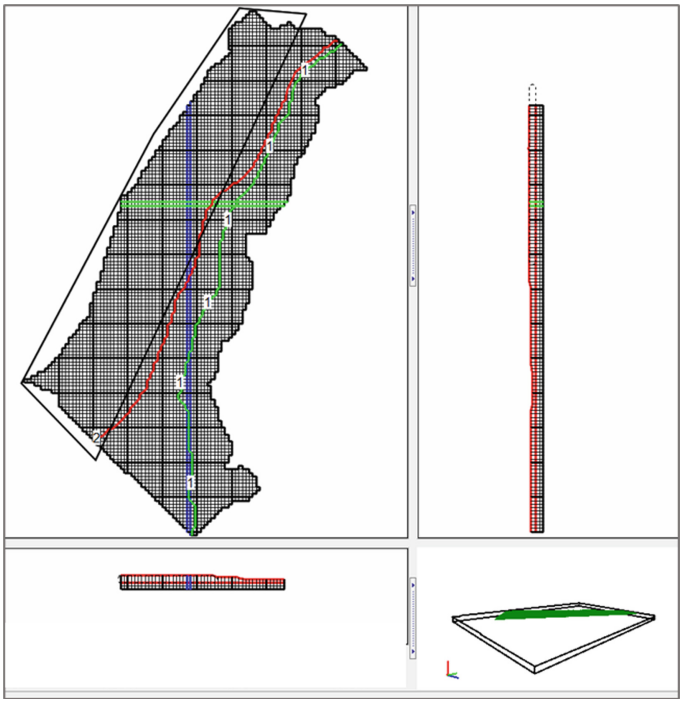

Fig. 5. MODFLOW model for the inland aquifer. View of the model through the ModelMuse interface. Topographical contour lines are also visualized.

tenth of horizontal conductivity. Hydraulic conductivity, specific storage, specific yield, and porosity were used calibrating parameters.

The MODFLOW-Newton (MODFLOW-NWT) solver was used in this research because it was considered more appropriate to model groundwater processes of an unconfined aquifer such as the Biscayne aquifer. This solver is commonly used to simulate groundwater flow involving wetting and drying under unconfined groundwater-flow conditions. MODFLOW-NWT was used with the Upstream-Weighting (UPW) Package for calculating intercell conductance.

Total simulation time was 4 years (2014–2017), being year 2014 used for model warm-up, i.e., results from the modeling process correspond to years 2015 to 2017. Stress periods of 86400 s were implemented for recharge data (input) and groundwater flow (output data). Total number of stress periods was 1463, representing 4 years. Therefore, currently the model generates daily groundwater flow data, although it can also generate hourly output. However, processing time and output visualization of hourly data was proven to be time-wise inefficient.

Indirect Calibration Based on Coastal Salinity

Since there are not observed data of groundwater at Biscayne Bay coast, the groundwater model was indirectly calibrated by inputting the MODFLOW output in an existing hydrodynamic and salinity model of Biscayne Bay (detailed in [15]). The hydrodynamic model computes hourly salinity at any location within Biscayne Bay. The MODFLOW model was calibrated by exploring if the MODFLOW-generated groundwater flows, when those flow were input to the hydrodynamic model, would produce salinity concentrations statistically similar to observed salinities. Observed hourly salinity data at stations BISC C4, BISC C6, and BISC D4, for years 2014 through 2017 were compared.

The measurement of how well predicted salinities matched observations was performed using several statistical indicators (Table 1). The goodness of fit was statistically assessed by the computation of the correlation coefficient (R), coefficient of determination (R^2), Nash Sutcliffe coefficient (NSE), Kling-Gupta efficiency (K-G), and Willmott's index of agreement (d). The bias of predicted salinity concentrations with respect to observed data was determined by the percent bias coefficient (PBIAS). These indicators are widely used to assess hydrological and water quality modeled output [17–19]. Table 3 also shows the acceptability ranges recommended by the cited literature.

Table 1. Statistical indicators of fit and acceptability ranges.

Indicators of fit	Formulae	Range
Percent bias, *PBIAS*	$\frac{\sum_{i=1}^{n}(Y_i^{Obs}-Y_i^{Sim})*100}{\sum_{i=1}^{n}(Y_i^{Obs}).}$	$< \pm 18\%$
Correlation coefficient, *R*	$\sqrt{\frac{\sum_{i=1}^{n}(Y_i^{Sim}-Y_i^{Mean}).^2}{\sum_{i=1}^{n}(Y_i^{Obs}-Y_i^{Mean}).^2}}$	> 0.71
Coefficient of determination	R^2	> 0.50
Nash–Sutcliffe efficiency, *NS*	$1-\frac{\sum_{i=1}^{n}(Y_i^{Obs}-Y_i^{Sim}).^2}{\sum_{i=1}^{n}(Y_i^{Obs}-Y_i^{Mean}).^2}$	> 0.50
Kling-Gupta efficiency, *K-G*	$1-\sqrt{\left(\frac{Y_{Sim}^{Mean}}{Y_{Obs}^{Mean}}-1\right)^2+\left(\frac{STDEV_{Sim}}{STDEV_{Obs}}-1\right)^2+(R-1)^2}$	> 0.50
Willmott's index of agreement, *d*	$1-\frac{\sum_{i=1}^{n}(Y_i^{Obs}-Y_i^{Sim}).^2}{\sum_{i=1}^{n}(\lvert Y_i^{Sim}-Y_{Obs}^{Mean}\rvert+\lvert Y_i^{Obs}-Y_{Obs}^{Mean}\rvert).^2}$	> 0.65
Y_i^{Obs} = Observed salinity Y_i^{Sim} = Simulated salinity Y_{Obs}^{Mean} = Mean of observed salinity Y_{Sim}^{Mean} = Mean of simulated salinity n = Total number of hourly salinity data		

3 Results

3.1 Calibration Phase

Table 2 Summarizes the main MODFLOW parameters resulting from the calibration phase. The parameter values shown in the table were selected from sensitivity analysis, where each parameter was varied until the model produced predictions of salinity concentrations (for the control salinity stations) that matched observed concentrations.

As shown in Table 2, a relatively high horizontal hydraulic conductivity (0.007 m/s) was implemented in the model. The adopted value is consistent with karst hydraulic conductivities published in the literature [20,21]. All other parameters were varied until salinity estimations produced by the hydrodynamic model matched observed salinity values. Adopted porosity and specific storage are consistent with values reported in the literature [22].

Figure 6 shows MODFLOW-estimated groundwater flows at the control stations (BISC C4, BISC C6, BISC D4).

Groundwater flow hydrographs at control stations are very similar (Fig. 6). Peak flows, however, vary depending on the station location. The highest groundwater flow

Table 2. Resulting MODFLOW calibration parameters

Feature	Adopted value
Number of layers	3
Layer depth	2 m
Horizontal hydraulic conductivity	0.007 m/s
Vertical hydraulic conductivity	7E−4 m/s
Specific storage	0.003
Initial head	Saturated
Porosity	0.25
Specific yield	0.2
Number of stress periods	1463
Stress period length	86400 s

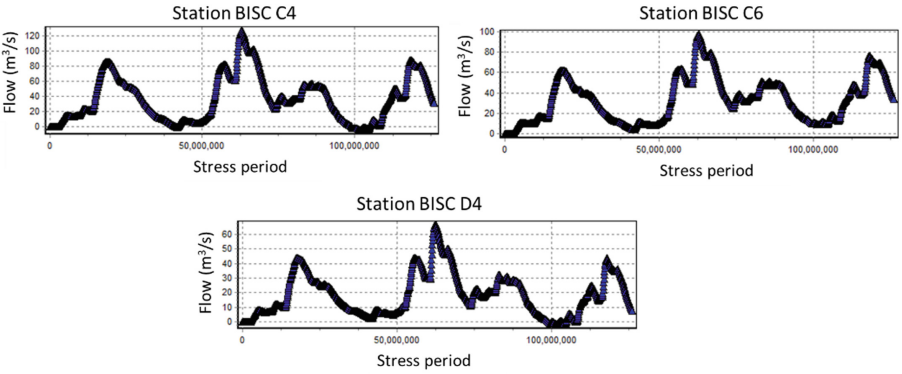

Fig. 6. Groundwater flows at control stations BISC C4, BISC C6, and BISC D4.

is estimated to occur at BISC C4 (130 m^3/s), and the lowest peak flow corresponds to BISC D4 (70 m^3/s). Since stations BISC C6 and BISC D4 are located farther east than BISC C4, i.e., farther from the recharge zone, these results were expected.

3.2 Salinity at Biscayne Bay's Central Coast

As stated in previous sections, the MODFLOW model output was input into an existing hydrodynamic and salinity model that predicts hourly salinity concentrations the control stations for years 2015 through 2017. Figure 7 shows a comparison of observed salinities at the control stations (BISC C4, BISC C6, and BISC D4), salinity estimation by the hydrodynamic model without groundwater inputs, and estimated salinities with groundwater inputs (generated by MODFLOW).

As shown in Fig. 7, when the hydrodynamic model does not account for groundwater contributions, salinity estimations (red line) fail to replicate the low observed salinities

during years 2016 and 2017 (blue line). As shown, salinities in the range of 5 PSU to 20 PSU were observed during those years (blue line). When groundwater contributions (estimated by MODFLOW) are taken into account, those low salinities are captured at the control stations. Also, inputting groundwater flows allows capturing the salinity temporal dynamics better than the hydrodynamic model.

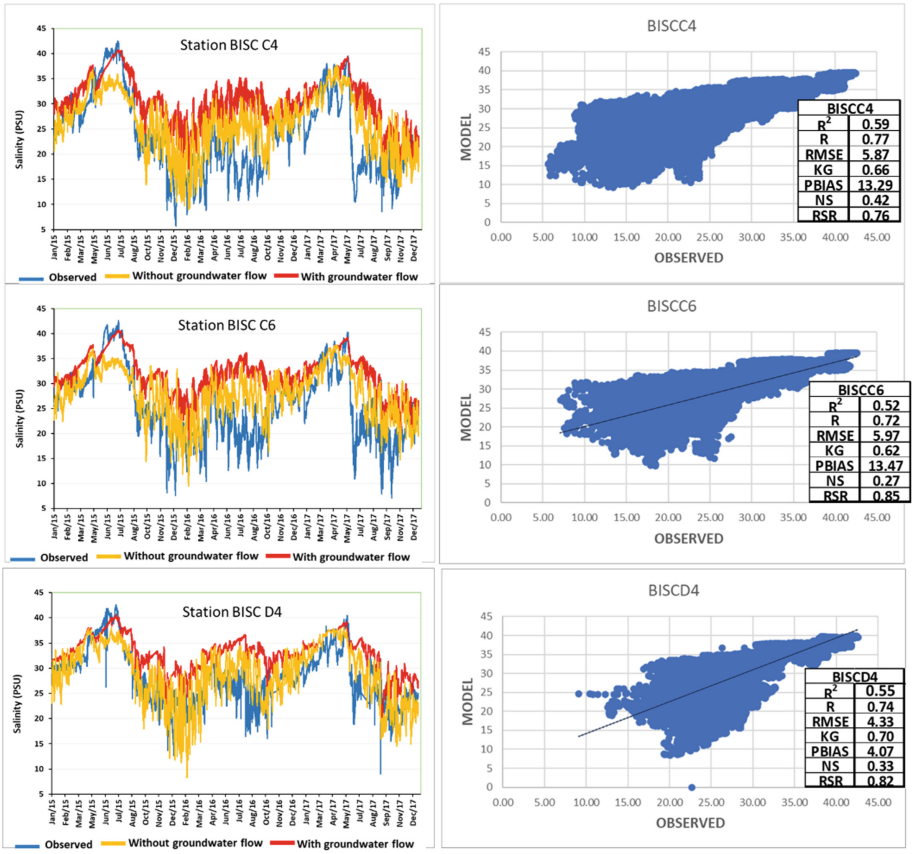

Fig. 7. Comparison of observed and simulated salinity for years 2015 to 2017. Simulated and observed hourly salinity concentrations at stations BISCC4, BISCC6, and BISCD4 are compared (Color figure online).

A statistical comparison of estimated salinities against observed salinities was performed. The goodness of fit indicators described in Table 1 (and shown in Fig. 8) were calculated to determine if the introduction of groundwater flows (calculated by the MODFLOW model) are actually beneficial to characterize the salinity regime at central Biscayne Bay.

As evidenced in Figs. 7 and 8, and Table 3, the MODFLOW groundwater model developed in this research allows simulating hourly salinity concentration values and trends (for years 2015 through 2017) well. When the hydrodynamic model does not

account for groundwater inputs (Table 3), 14 statistical indicators of fit (out of 18) are outside acceptability ranges (78%). When groundwater contributions calculated by MODFLOW are introduced to the hydrodynamic model, only 5 out of 18 statistical indicators are not within acceptability ranges (28%). Half of the statistical indicators corresponding to BISC C6 (when groundwater is accounted for) are not optimal. The indicators that are out of acceptability range correspond to statistics that are very sensitive to extreme values (R^2, NSE). The extreme salinity peak observed in July 2015, that is not captured in the salinity simulations could be the reason for the disagreement between observed and simulated salinities. Regardless of the limited 2015 simulation, the statistical indicators were substantially improved for all observed/simulated comparisons (Table 3).

Table 3. Comparison of statistical indicators of fit.

Indicator	R	R^2	K-G	NSE	d	PBIAS	Station
Acceptability range	>0.71	>0.5	>0.5	>0.5	>0.65	<±18%	
No groundwater	0.66	0.44	0.42	−0.25	0.56	−26.4%	BISC C4
With groundwater	0.77	0.59	0.66	0.42	0.81	13.3%	
No groundwater	0.65	0.42	0.40	−0.41	0.51	−24.9%	BISC C6
With groundwater	0.72	0.52	0.62	0.27	0.76	13.5%	
No groundwater	0.74	0.55	0.56	−0.23	0.62	−16.4	BISC D4
With groundwater	0.74	0.55	0.70	0.33	0.83	4.1%	

The statistical indicators corresponding to the hydrodynamic model without groundwater are mostly outside of acceptability ranges: $0.65 < R < 0.74$; $0.42 < R^2 < 0.55$; K-G < 0.56; d < 0.62; −26.4 < PBIAS < −16.4 (Table 5). The indicators corresponding to the salinities estimated with MODFLOW groundwater inputs show acceptable goodness of fit ($0.72 < R < 0.77$; $0.52 < R^2 < 0.59$; $0.62 < K\text{-}G < 0.70$; $d > 0.76$) and statistical bias (4.1% < PBIAS < 13.5%).

4 Conclusions

In this research, a MODFLOW groundwater model for central Biscayne Bay (Florida, USA) allowed successful simulation of hourly salinity concentrations for 3-years (2015 through 2017). Salinities calculated by an existing hydrodynamic/salinity model using groundwater inputs calculated by MODFLOW were statistically compared to observed salinities at three coastal salinity stations located in central Biscayne Bay: BISC C4, BISC C6, and BISC D4. Calibration of the groundwater model was performed by inputting the MODFLOW output in an existing hydrodynamic and salinity model of Biscayne Bay. The hydrodynamic model computed hourly salinity at the control stations explored in this research. The MODFLOW model was considered calibrated when model-generated

groundwater flows produced salinity concentrations statistically similar to observed salinities.

Statistical indicators of goodness of fit show that the MODFLOW groundwater flows can improve the estimation of salinities at the central coast of Biscayne Bay. Loosely linking the MODFLOW outputs to a hydrodynamic model improved salinity estimations performed by the hydrodynamic model allowed a 50% improvement in the quality of statistical fit. The groundwater model could be improved in capturing salinity peaks occurring during year 2015. However, in its current form the MODFLOW-hydrodynamic model combination allows better simulation of salinity concentrations and trends, than an existing hydrodynamic model without groundwater inputs.

The methodology presented in this paper have the potential to be applied to other coastal locations in the Florida Peninsula and elsewhere in which karst terrain is predominant and groundwater contributions are unknown.

References

1. Ye, Q., Li, Z., Duan, L., Xu, X.: Decoupling the influence of vegetation and climate on intra-annual variability in runoff in karst watersheds. Sci. Total Environ. **824** (2022). https://doi.org/10.1016/j.scitotenv.2022.153874
2. Hollingsworth, E.: Karst regions of the world (KROW): populating global karst datasets and generating maps to advance the understanding of karst occurrence and protection of karst species and habitats worldwide. Thesis, University of Arkansas (2006). https://digital.lib.usf.edu/SFS0052617/00001
3. Upchurch, S., Scott, T.M., Alfieri, M., Fratesi, B., Dobecki, T.L.: The Karst Systems of Florida: Understanding Karst in a Geologically Young Terrain, pp. 1–15. Springer, Cham (2019). https://doi.org/10.1007/978-3-319-69635-5
4. Bahtijarevic, A.: Karst landforms in Florida, Geomorphological analysis. Thesis, Department of Geology, University of South Florida (1996)
5. Klammler, H., Jawitz, J.W., Annable, M.D., Yaquian, J.A., Hatfield, K., Burger, P.: Decadal scale recharge-discharge time lags from aquifer freshwater-saltwater interactions. J. Hydrology, **582** (2020). https://doi.org/10.1016/j.jhydrol.2019.124514
6. Conrads, P.A., Darby, L.S.: Development of a coastal drought index using salinity data. Bull. Am. Meteor. Soc. **98**, 753–766 (2017). https://doi.org/10.1175/BAMS-D-15-00171.1
7. Alarcon, V.J., Linhoss, A.C., Kelble, C.R., Mickle, P.F., Bishop, J., Milton, E.: Estimation of hourly salinity concentrations using an artificial neural network. In: Gervasi, O., et al. (eds.) ICCSA 2021. LNCS, vol. 12954, pp. 629–640. Springer, Cham (2021). https://doi.org/10.1007/978-3-030-86979-3_44
8. Orlando, S.P.Jr., Rozas, L.P., Ward, G.H., Klein, C.J.: Salinity Characteristics of Gulf of Mexico Estuaries. Silver Spring, MD, National Oceanic and Atmospheric Administration, Office of Ocean Resources Conservation and Assessment (1993). 209 pp.
9. Caccia, V., Boyer, J.: Spatial patterning of water quality in Biscayne Bay, Florida as a function of land use and water management. Mar. Pollut. Bull. **50**, 1416–1429 (2005). https://doi.org/10.1016/j.marpolbul.2005.08.002
10. Fernald, E.A., Purdum, E.: Water Resources Atlas of Florida. Institute of Science and Public Affairs, Florida State University (1998). https://fga.freac.fsu.edu/gaw/2001/resources/waterpdf/biscayne_aquifer.pdf
11. Miller, J.A.: Ground Water Atlas of the United States: Alabama, Florida, Georgia, South Carolina. U.S. Geological Survey, Publication HA 730-G (1990). https://www.nrc.gov/docs/ML1002/ML100290484.pdf

12. Weyer, K.U.: The case of the Biscayne Bay and aquifer near Miami, Florida: density-driven flow of seawater or gravitationally driven discharge of deep saline groundwater? Environ. Earth Sci. **77**(1), 1–16 (2017). https://doi.org/10.1007/s12665-017-7169-5
13. USGS: Changing Salinity Patterns in Biscayne Bay, Florida. Prepared in cooperation with South Florida Water Management District and Biscayne National Park (2004). https://doi.org/10.3133/fs20043108
14. Stalker, J., Price, R., Swart, P.: Determining spatial and temporal inputs of freshwater, including submarine groundwater discharge, to a subtropical estuary using geochemical tracers, Biscayne bay South Florida. Estuaries Coasts **32**, 694–708 (2009). https://doi.org/10.1007/s12237-009-9155-y
15. Alarcon, V.J., Linhoss, A.C., Kelble, C.R., et al.: Coastal inundation under concurrent mean and extreme sea-level rise in Coral Gables, Florida, USA. Nat Hazards **111**, 2933–2962 (2022). https://doi.org/10.1007/s11069-021-05163-0
16. USGS. ModelMuse: A Graphical User Interface for Groundwater Models (2022). https://www.usgs.gov/software/modelmuse-graphical-user-interface-groundwater-models
17. Moriasi, D.N., Arnold, J.G., Van Liew, M.W., Bingner, R.L., Harmel, R.D., Veith, T.L.: Model Evaluation Guidelines for Systematic Quantification of Accuracy in Watershed Simulations. Trans. ASABE, **50**, 885–900 (2007). https://doi.org/10.13031/2013.23153
18. Ang, R., Oeurng, C.: Simulating streamflow in an ungauged catchment of Tonlesap Lake Basin in Cambodia using Soil and Water Assessment Tool (SWAT) model. Water Sci. **32**, 89–101 (2018). https://doi.org/10.1016/j.wsj.2017.12.002
19. Knoben, W.J.M., Freer, J.E., Woods, R.A.: Technical note: Inherent benchmark or not? Comparing Nash-Sutcliffe and Kling-Gupta efficiency scores. Hydrol. Earth Syst. Sci. **23**, 4323–4331 (2019). https://doi.org/10.5194/hess-23-4323-2019
20. Schrader, A., Erasmus, E., Winde, F.: Determining hydraulic parameters of a karst aquifer using unique historical data from large-scale dewatering by deep level mining - a case study from South Africa (2014). Water SA. https:// doi.org/40 .555.10.4314/wsa.v40i3.20
21. Kovács, A.: Geometry and hydraulic parameters of karst aquifers: a hydrodynamic modeling approach (2003). Ph.D. dissertation, Université de Neuchâtel, Switzerland, p 1724 (2003)
22. Kuang, X., Jiao, J.J., Zheng, C., Cherry, J.A., Li, H.: A review of specific storage in aquifers. J. Hydrol. **581** (2020). https://doi.org/10.1016/j.jhydrol.2019.124383